BULLETIN OF THE POLISH ACADEMY OF SCIENCES
TECHNICAL SCIENCES
DOI: 10.24425/bpasts.2024.149175

The effect of magnesium and copper addition on the microstructure, mechanical properties and corrosion rate of as-cast biodegradable zinc alloys

M. Gieleciak[1*], K. Janus[1,2], Ł. Maj[1], P. Petrzak[1], M. Bieda[1], A. Jarzębska[1*]

[1]Institute of Metallurgy and Materials Science, Krakow, Poland
[2]Faculty of Foundry Engineering, AGH University of Science and Technology, Krakow, Poland

Abstract. Microstructure, mechanical and corrosion properties of as-cast pure zinc and its binary and ternary alloys with magnesium (Mg), and copper (Cu) additions were investigated. Analysis of microstructure conducted by scanning electron microscopy revealed that alloying additives contributed to decreasing average grain size compared to pure zinc. Corrosion rate was calculated based on immersion and potentiodynamic tests and its value was lower for materials with Cu content. Moreover, it was shown that the intermetallic phase, formed as a result of Mg addition, constitutes a specific place for corrosion. It was observed that a different type of strengthening was obtained depending on the additive used. The presence of the second phase with Mg improved the tensile strength of the Zn-based materials, while Cu dissolved in the solution had a positive effect on their elongation.

Key words: biodegradable zinc alloys, alloying additives, mechanical properties, microstructure, corrosion rate

1. INTRODUCTION

Recently, zinc has gained in popularity in the context of medical applications for temporary biodegradable implants [1–5]. The fact that zinc is an essential element for the human body, responsible for several biological functions such as cell proliferation or apoptosis regulation further increases this attention [6,7]. What is more, pure zinc has an optimal degradation rate in terms of use as a potential material for biodegradable cardiovascular stents, compared to magnesium (which corroding too quickly) and iron (which corrodes too slowly) [7]. However, such use is prevented by pure zinc's low mechanical properties. Overcoming the limitation is possible thanks to zinc-based alloys with magnesium, copper, calcium, silver or other biocompatible elements [8]. Even small amounts such as 0.1 wt.% of Mg improves the strength of pure zinc almost three-fold, reaching ultimate tensile strength (UTS) of 81.5 MPa. A further increase of Mg content up to 0.8 wt.% results in a constant increase of yield strength (YS) and UTS, reaching 112 MPa and 120 MPa, respectively [9]. Such an improvement is associated with grain boundary strengthening, since 0.1 wt.% of magnesium addition led to grain refinement from 3094 ± 84 μm (for pure Zn) to 160 ± 22 μm. Further increase of Mg had a beneficial effect on grain size reduction, and finally 65 ± 9 μm for 0.8 wt.% was obtained [9]. Based on the literature reports, it seems that the threshold for Mg content is 2%. Above this value, the deterioration of properties can be observed. For example, addition of 1 wt.% of Mg [3] caused growth of YS and UTS to about 100 MPa and 150 MPa, 1.2 wt.% [10] to 116.5 ± 1.2 MPa, 129.6 ± 6.4 MPa, 1.6 wt.% [11] to UTS 172 ± 12 MPa, while a 3 wt.% decrease of YS and UTS to 65 ± 9 MPa and 84 ± 9 MPa [12], respectively were achieved. While it is known that Mg can strengthen the Zn-based alloy, it has no positive effect on the elongation (A) of the alloys, as with addition of up to 0.8 wt.% the elongation stayed below 1%. Moreover, when studying its effect on corrosion rate there is no linear trend indicating that increasing the amount of Mg improves or weakens corrosion resistance [13]. One report [14] focusing on other as-cast binary zinc alloys indicates that copper addition up to 4 wt.% does not significantly affect grain refinement and elongation, but did improve UTS from 9.5 MPa for pure zinc to 105.4 MPa for Zn-4Cu. Immersion testing in HBSS performed over periods of five to 40 days revealed better corrosion resistance over longer time for all investigated Zn-xCu alloys. Combining several alloying additives and creating ternary alloys may bring positive effects in terms of mechanical properties and corrosion rates, both of which are important factors for the potential application of zinc alloys as temporary implants. Zn-Mg-Sr alloys [15] with YS and UTS 129.08 ± 5.07 MPa and 144.15 ± 14.97 MPa, respectively, are an example of this. Manganese addition to Zn-Mg alloy [2] can also increase YS and UTS, yet at the expense of elongation. Moreover, that alloy exhibits significantly higher corrosion resistance compared to pure Zn. Attempts have also been made to create biodegradable ternary alloys with Ti [16] and Ca [17] additions in Zn-Cu and Zn-Mg, respectively. Micro-alloying (0.05 wt.%) of titanium led to improved mechanical properties, but a greater amount (0.1 wt.%) worsened these parameters. Moreover, corrosion rate increased due to Ti addition. For Zn-1.5Mg-0.1Ca, YS, UTS and A improvements reaching 173.8 ± 15.1 MPa, 241.4 ± 0.4 MPa and 1.72 ± 0.01 %,

*e-mail: m.gieleciak@imim.pl, a.jarzebska@imim.pl

respectively, were achieved. Therefore, it seems that three-component alloys bring better results in the as-cast state than binary materials. However, selecting the appropriate elements, which will contribute to increased strength and elongation while maintaining the optimal degradation rate of pure Zn still requires investigation.

Thus, the main aim of this work is to design a Zn-Mg-Cu ternary alloy and indicate the effect of magnesium and copper addition on the mechanical and corrosion properties in as-cast state. The proposed systematic comparison of pure Zn with binary Zn-Mg and Zn-Cu, and finally ternary Zn-Mg-Cu alloy in as-cast state, will contribute to better understanding of the effect of particular elements on the microstructure and properties of Zn-based alloys, and thus to the more efficient creation of new materials for medical use as temporary implants.

2. MATERIALS AND METHOD

Pure zinc and its alloys, with 1 wt.% of copper, 0.8 wt.% of magnesium, and with 0.8 wt.% of magnesium and 0.2 wt.% of copper (denoted as Zn, ZnCu, ZnMg and ZnMgCu, respectively) were used for the investigation. Zinc (purity of 99.99%), magnesium (purity of 99.99%) and CuZn40 brass were gravity casted in an argon atmosphere at 650°C. As a result, ingots with 75mm diameter and 200mm height were obtained. Microstructural characterisation was done with FEI E-SEM XL30 scanning electron microscope equipped with an energy dispersive spectrometer (EDS) EDAX Genesis. Samples were ground using abrasive papers from 220 to 7000 grit, polished by 1 µm and ¼ µm diamond suspensions and electropolished with C1 electrolyte under the following conditions: voltage 25 V and time 15 seconds. Additionally, Zn and ZnCu were etched with a 4% nital solution in order to reveal microstructural features. ImageJ software was used for further microstructural characterisation. To confirm the phase composition, X-ray diffraction (XRD) was performed by using Bruker D8 Discover. Corrosion properties were tested by electrochemical and immersion tests. Cubic samples with an area exposed to Hanks' Balanced Salt Solution (HBSS) of 0.29 and 1.7cm^2, respectively, for electrochemical and immersion tests were prepared on abrasive papers up to 7000. Potentiodynamic curves were recorded with the use of an Autolab PGSTAT 302 potentiostat and Nova 2.1.4 software. Three measurements were taken for each material, and the average corrosion rate was calculated according to ASTM G31-72. Static immersion tests (IT) were conducted for 24 and 120 hours in HBSS. For this test, four cubic samples from each material were immersed separately in 50ml of HBSS, in sterile containers that were placed in an incubator at 37°C. After every 48h, the corrosion medium was changed to maintain the pH at 7.4. After the immersion test, the samples were weighed with corrosion products, and then cleaned in ammonium chloride heated to 70°C for 20 minutes and five minutes in ethanol to remove the corrosion products and weighed again. Based on this, the corrosion rate was calculated according to ASTM G102-89. Mechanical properties were designated by static tensile test on the Instron 6025 modified by a Zwick Roell machine at room temperature (22°C). Three samples of each material with 3mm diameter and 14mm gauge length (Fig. 1) were tested at a strain rate of 10^{-3} s^{-1}.

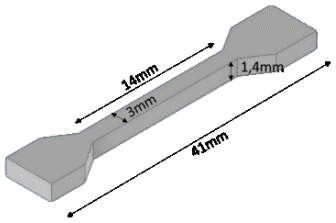

Fig.1. Example of the specimen used for static tensile test

3. RESULTS

A. Microstructural characterisation

Microstructure images obtained by scanning electron microscope are presented in Fig. 2. Pure zinc was characterised by large, equiaxed α-Zn grains. Twins observed in the microstructure appeared most likely as a result of the metallographic section preparation. Also in the case of ZnCu, equiaxed grains of η-Zn were distinguished, suggesting that the alloying additive is fully dissolved in the solid solution. Materials with magnesium addition consist of α-Zn grains and eutectic mixture composed of α-Zn and intermetallic phase Mg_2Zn_{11} located along the Zn grains boundaries. Microstructure of ternary alloy appeared to be similar to Zn-Mg alloy, however, due to Cu addition, consisted of η-Zn instead of α-Zn. Based on ImageJ software, average grain sizes of investigated casts were calculated. Data revealed that alloying additives allowed a significant grain refinement, and that magnesium rather than copper addition contributes best to this (Fig. 3). Pure Zn in the as-cast state has the highest average grain size (approximately 1100 µm), while addition of as little Mg as 0.8 wt.% resulted in an almost ten-fold decrease in the average grain size.

Further alloying with 0.2 wt.% of Cu, resulting in ternary ZnMgCu, caused a further decrease, to 130±63µm. Additionally, for ZnMg and ZnMgCu alloys, the percentage fraction of the intermetallic Mg_2Zn_{11} phase was calculated. Despite the same amount of Mg addition to alloys, a higher fraction of the phase was calculated for ZnMgCu due to the differences in Zn content in these alloys (99.2 vs 99.0 wt.%, respectively) (Table 1).

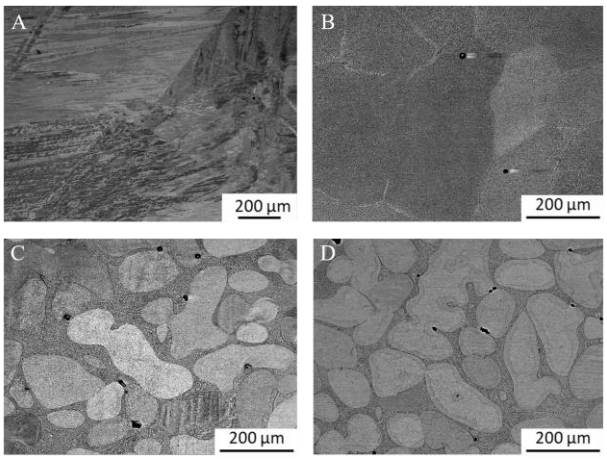

Fig.2. Microstructures of A) Zn, B) ZnCu, C) ZnMg, D) ZnMgCu. obtained in backscattered electron (BSE) mode

Table 1. Average grain size and fraction of intermetallic phase of investigated casts

Material	Average Grain Size [µm]	Fraction of Mg_2Zn_{11} [%]
Zn	1100	-
ZnCu	433 ± 147	-
ZnMg	145 ± 81	14
ZnMgCu	130 ± 63	18

With the EDS and XRD techniques, it was possible to carry out qualitative analysis of the chemical composition of alloys. Diffractograms are presented in the Fig. 4, and the distribution of the elements through the mapping by EDS in Fig. 5. It was confirmed that, regardless of the material, magnesium was located primarily in the eutectic mixture with negligible amounts dissolved in α-Zn grains, while copper locates as a solute element both in materials where Cu content is higher, at 1 wt.% in binary ZnCu alloy, and when it is a minor additive of 0.2 wt.% in ternary ZnMgCu, without the formation of any intermetallic phases. For the latter material, the presence of Cu was noticed mainly in the η-Zn matrix and diminished in the area of the intermetallic phase, suggesting its minor solubility.

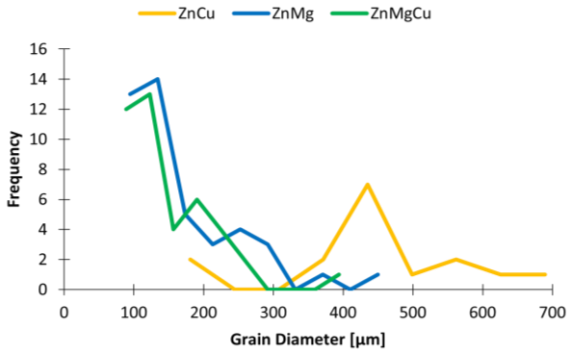

Fig.3. Grain size distribution of investigated alloys

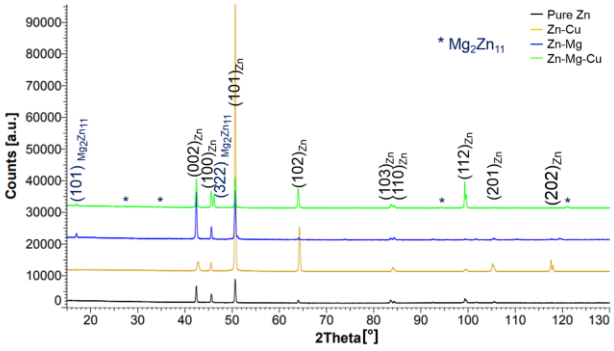

Fig.4. X-ray diffractograms obtained for analysed materials

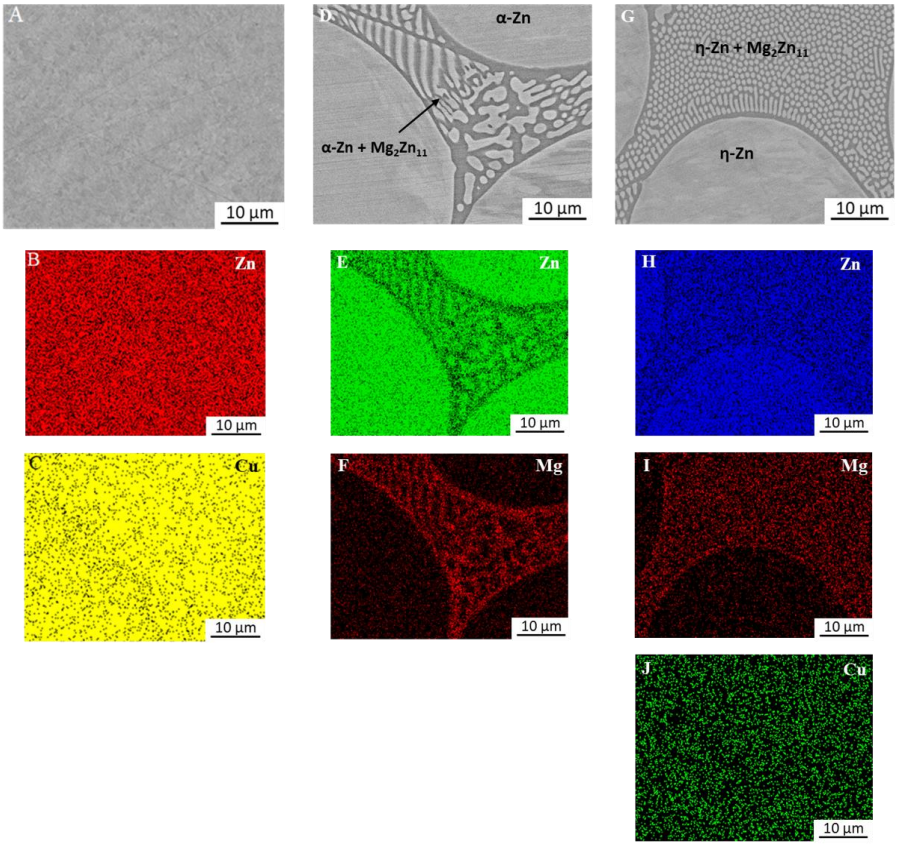

Fig.5. SEM/BSE images of A) ZnCu alloy with distribution maps of B) Zn, C) Cu, D) ZnMg alloy with distribution maps of E) Zn, F) Mg, and G) ZnMgCu alloy with distribution maps of H) Zn, I) Mg and J) Cu

B. Corrosion properties

The two-step corrosion rate investigation was started with electrochemical tests. Table 2 presents the average values of the main parameters obtained from the potentiodynamic test. Corrosion potential (E_{Corr}) for Zn and ZnMgCu was at the same level -0.943 V. For binary Zn-based alloys, a significant shift of E_{Corr} (as compared with pure Zn) was observed for more noble values (-0.931 V) when copper was added, while for magnesium addition E_{Corr} decreased to -0.970 V. Those results are in agreement with obtained current density (J_{Corr}) and in consequence corrosion rate (V_{Corr}).

Pure Zn and ternary alloy possessed V_{Corr} at a similar level (0.36 and 0.38 mm/year, respectively). In the case of ZnCu, compared to pure zinc, a decrease in V_{corr} was observed, achieving 0.31 mm/year. The highest degradation rate of 0.4 mm/year was obtained in the case of the ZnMg. The changes in corrosion rate in the function of chemical composition are presented in Fig. 6. It is worth highlighting that the ternary alloy, of a composition proposed and designed for the first time in this work, has a corrosion rate comparable (within the measurement error) to initial pure Zn material even if any of the additive itself results in significant changes in this property.

TABLE 2. Average values of potentiodynamic test parameters

Material	Corrosion potential [V]	Current density [μA/cm^2]	Corrosion rate [mm/year]
Zn	-0.943 ± 0.02	20 ± 2	0.36 ± 0.06
ZnCu	-0.931 ± 0.01	18.4 ± 4	0.31 ± 0.04
ZnMg	-0.970 ± 0.01	21.2 ± 3	0.40 ± 0.08
ZnMgCu	-0.943 ± 0.01	20.7 ± 3	0.38 ± 0.07

In order to deepen understanding of the alloying element effect on corrosion properties, a static immersion test (IT) was performed. Table 3 presents a summary of the mass of corrosion products, mass loss calculated as a difference between initial mass of the samples and the weight of the samples after removing corrosion products and the corrosion rate determined based on mass loss. After 24h of IT in HBSS, similar results in terms of degradation rate were achieved and stayed in the range of 0.14 – 0.22 mm/year. However, the tendency of alloys with Cu addition to exhibit higher mass loss and in consequence higher V_{corr} as compared to pure Zn and the ZnMg alloy was observed for the first 24h. Prolonged time of immersion (120h) caused, regardless of chemical composition, a significant decrease in corrosion rate, of about one order of magnitude (Fig.7). Moreover, after 120h a rather

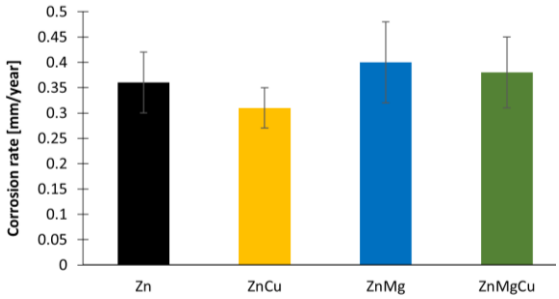

Fig.6. Corrosion rate determined from electrochemical test

opposite trend was noticed, as the ternary alloy showed the slowest degradation rate, and pure Zn the fastest. Based on the obtained results, one should conclude the following: for longer duration of immersion, magnesium inhibits the degradation of Zn-based alloys to a much greater extent than copper. In all the investigated cases, except the pure Zn, prolonged immersion time resulted in the formation of larger amounts of corrosion products.

TABLE 3. Average values of corrosion products, mass loss and corrosion rate after static immersion

Material	Mass of corrosion products [mg]		Mass loss [mg]		Corrosion rate [mm/year]	
	24h	120h	24h	120h	24h	120h
Zn	0.29 ± 0.1	0.29 ± 0.2	0.44 ± 0.2	0.99 ± 0.4	0.15 ± 0.05	0.067 ± 0.029
ZnCu	0.27 ± 0.2	0.34 ± 0.1	0.60 ± 0.1	0.80 ± 0.1	0.20 ± 0.01	0.054 ± 0.006
ZnMg	0.24 ± 0.1	0.33 ± 0.1	0.42 ± 0.1	0.67 ± 0.1	0.14 ± 0.02	0.045 ± 0.006
ZnMgCu	0.17 ± 0.1	0.52 ± 0.1	0.64 ± 0.1	0.55 ± 0.1	0.22 ± 0.04	0.038 ± 0.007

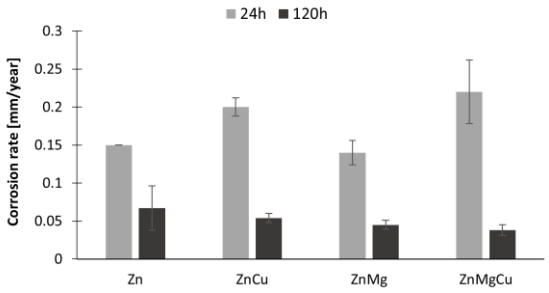

Fig.7. Corrosion rate determined from static immersion test for 24h and 120h

SEM observations of sample surfaces exposed to HBSS suggest that after 24h a discontinuous corrosion products layer was formed. The morphology was similar for each material. Over time, the number of products increased, which correlates with data obtained from mass measurements. After 120h, a compact layer of corrosion products distributed evenly on the surface was visible in all investigated materials. Examples of the sample surface exposed to HBSS after the different immersion time are given in Fig. 8. After the cleaning procedure of corrosion products, SEM images indicate that some of them were still present on the surface. This was especially true for Zn and ZnMg. In two other cases, i.e., ZnCu and ZnMgCu, scratches and single corrosion products were noticeable. For samples after 120h of IT, products after cleaning were less pronounced and SEM images provided more information.

As regards pure Zn, the presence of large pits and detachment of substantial portions of the material were observed. In the case of the ZnMg and ZnMgCu, localised corrosion was seen, since in the area of the eutectic mixture an increased number of pits were noticed compared to the grain interior. Moreover, in all investigated cases, the number of pits increased with prolonged test duration. The least visible changes compared to the material before immersion were noticed for the ZnCu alloy. Further analysis conducted on cross-sections of the corrosion layer confirmed the calculated corrosion rates. Pure Zn and ZnCu alloy exhibited more developed surfaces with numerous pits compared to the alloys containing Mg (Fig. 9). This was in accordance with measured mass loss, where 0.99 and 0.80 mg weight decrease was achieved respectively for pure Zn and ZnCu alloy, which was higher by at least 13 mg than in the case of Mg-contented alloys. Moreover, it was noticed that alloying additives lead to increasing the corrosion layer thickness, compared to pure Zn. This effect was more pronounced in the case of Mg addition rather than Cu. The thick, dense layer of corrosion products was especially visible near the intermetallic phase. SEM observations were supported by measuring the average thickness of the corrosion layer using ImageJ (see Table 4). Chemical composition investigation from cross-sections of the corrosion product layer, after 120h of IT was performed using the EDS technique. This revealed that there was no significant difference in the chemical composition of the layer of corrosion products, regardless of alloying additives. In the majority, apart from Zn and alloying additives, the corrosion products layer consisted of oxygen (O), chlorine (Cl), calcium (Ca), and phosphorus (P). It was noticed that Cl and Mg tend to be located in some specific places, while Zn, O, Ca and P were distributed evenly in whole volume of the layer. The example of distribution of particular elements within the corrosion product layer is presented in Fig.10.

Table 4. Average corrosion layer thickness

Material	Average corrosion layer thickness [μm]
Zn	6 ± 1
ZnCu	5.5 ± 1
ZnMg	20 ± 4
ZnMgCu	22 ± 3

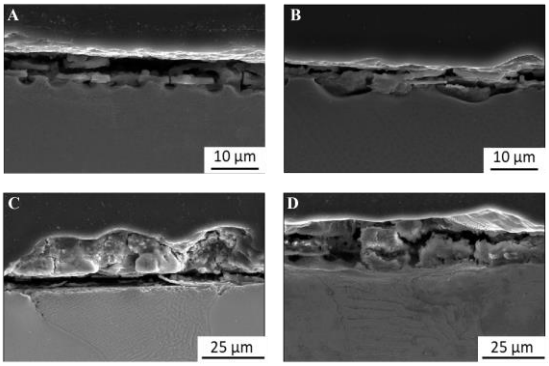

Fig.9. SEM/SE microstructures of corrosion product layer cross-section after 120h IT of A) pure Zn, B) ZnCu alloy, C) ZnMg alloy and D) ZnMgCu alloy

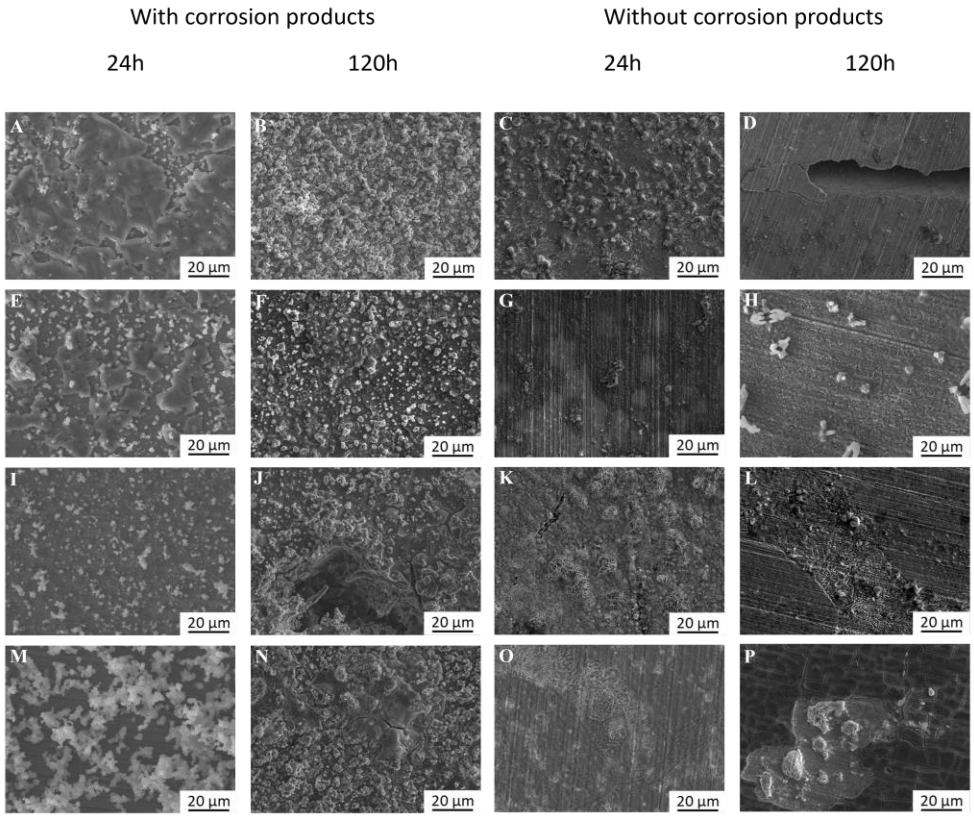

Fig.8. SEM/SE images samples surface after 24h and 120h of immersion test in HBSS and after removing the corrosion products for A-D) pure zinc; E-H) ZnCu; I-L) ZnMg; M-P) ZnMgCu

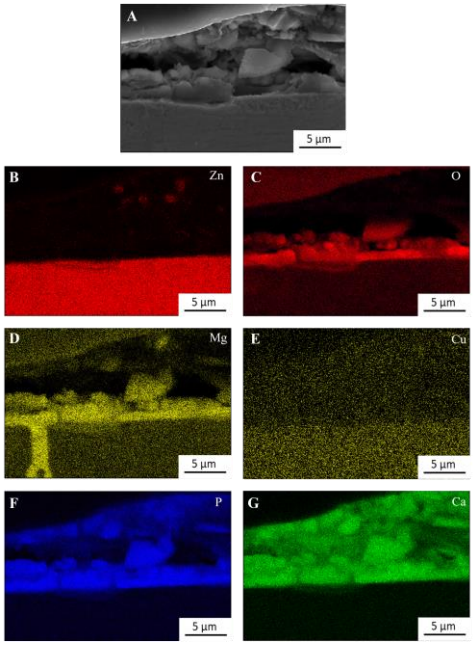

Fig.10. SEM/SE microstructures of corrosion product layer cross-section after 120h IT of ZnMgCu alloy A) with corresponding distribution of B) Zn, C) O, D) Mg, E) Cu, F) P and G) Ca

C. *Mechanical properties*

To establish how alloying additives affect mechanical properties of the Zn material, a static tensile test was performed. Based on stress-strain curves, presented in Fig. 9, average values of yield strength (YS), ultimate tensile strength (UTS) and elongation (A) were determined and listed (Table 5). In reference to [18] it was confirmed that pure Zn possesses very low mechanical strength expressed in YS and UTS of 10 MPa and 18 MPa, respectively, with elongation as low as 0.3%. Alloying Zn with low magnesium and/or copper content significantly increases not only mechanical strength but also elongation. Based on the results, one may conclude that the best combination of strength and elongation was obtained for the ZnMgCu, for which YS and UTS were as high as 54 MPa and 81 MPa, respectively, with A of 1.6%. The character of the stress-strain curves (Fig. 11) for alloys with Mg addition indicated brittleness of the materials, while ZnCu was more ductile.

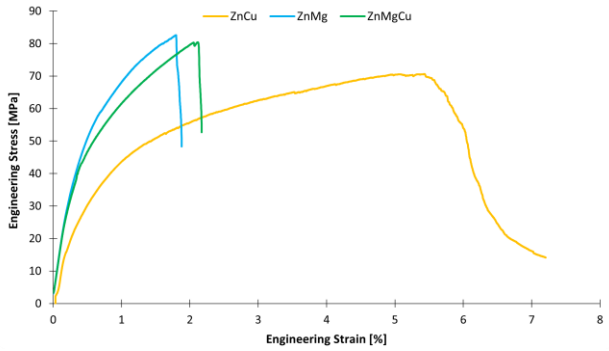

Fig. 11. Representative stress-strain curves from static tensile test

TABLE 5. Average mechanical properties values for the investigated materials

Material	YS [MPa]	UTS [MPa]	A [%]
Zn*	10	18	0.3
ZnCu	37 ± 5	69 ± 5	4.5 ± 0.7
ZnMg	53 ± 7	70 ± 8	1.4 ± 0.2
ZnMgCu	54 ± 4	81 ± 4	1.6 ± 0.7

* Results from the literature [18]

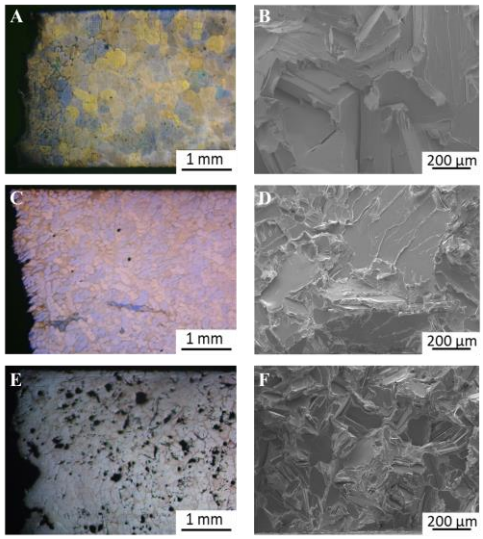

Fig. 12. Microstructure of A) ZnCu; C) ZnMg; E) ZnMgCu alloy after static tensile test and corresponding B),D),F) SEM/SE fractures

Similar properties were also observed during microstructure analysis of tensile tested samples. Optical microscopy observation of the surface of dog-bone samples confirmed the brittle fracture in alloys with magnesium addition. Zinc phase has a tendency to deform, and brittle cracking occurs in regions where eutectic mixture was present. In the case of ZnCu, the occurrence of twins was noticed on the surface, especially in close proximity to the cracked site (Fig.12). Moreover, SEM/SE observations of the fractures correspond well with other results, since an almost flat surface was observed in the case of ZnMg and ZnMgCu alloys, suggesting brittle fracture. Meanwhile, for ZnCu, a more developed surface with visible voids, indicating plasticity.

4. DISCUSSION

In this work, pure zinc, as a reference material, and three alloys (ZnCu, ZnMg and ZnMgCu) in as-cast state were characterised. Microstructural analysis indicated an effect of alloying additives, especially magnesium, on grain refinement. This is confirmed by the average grain size determination, which for pure zinc was over 1000 µm, for ZnCu about 430 µm, and for magnesium close to 150 µm. Based on the binary equilibrium phase diagrams of Zn-Mg one, it should be noted that addition of Mg even as low as 0.1 wt.% results in the formation of an Mg_2Zn_{11} intermetallic phase [9]. The volume fraction of Mg_2Zn_{11} of 14%, calculated in this work, forming the eutectic mixture, significantly inhibited the grain growth during the casting process [9,13]. This allows one to assume that, in order to obtain a fine-grained microstructure, it is more advantageous to select

chemical elements which form with zinc-based second phases [19]. In this way, the effect of Cu in the microstructure refinement is much less pronounced even with addition of 1 wt.%, which did not allow intermetallic phases to form (the maximum solubility of Cu in η-Zn is 2.7 wt.% according to the phase diagram [19]), and all the copper is substituted for the Zn atoms in its crystal structure. For ternary ZnMgCu alloy, the eutectic mixture (η-Zn+Mg_2Zn_{11}), formed at the grain boundaries of Zn grains, inhibits grain growth more efficiently than Cu dissolved in the Zn grains. Thus, the changes in the average grain size and resulting mechanical properties between ZnMg and ZnMgCu are negligible. Similar results can be observed in the literature [17], [20-24]. Based on the results of the electrochemical test, it can be concluded that the addition of copper increases the corrosion resistance of zinc, while magnesium causes its decrease. According to the electropotential series copper has +0.34 V and zinc -0.76 V, so Cu improves corrosion properties, while magnesium (-2.37 V) contributes to faster degradation [25, 26]. For this reason, the addition of copper to ZnMg led to a reduction in the corrosion rate value. However, this was not in correlation with the results obtained from the immersion test, where the list from last to most corrosion resistant was as follows: for 24h ZnMgCu > ZnCu > Zn > ZnMg and for 120h Zn > ZnCu > ZnMg > ZnMgCu. It should be underlined that, in the case of 24h IT, the degradation rate values were very similar. However, the discrepancy between corrosion rate assessed based on electrochemical and immersion tests is not unusual and already found in the literature [27]. It is more reasonable to determine corrosion rate based on immersion testing, because it is prolonged in time and closer to behaviour in the physiological environment. Moreover, the process is not forced by the polarisation of the sample. Results indicate that the grain size seems to be a crucial factor affecting corrosion rate [13]. Results from the static immersion test performed for 120h showed a clear correlation between grain size and corrosion rate (Fig. 13). Similar results were found in the literature [28, 29], where a decrease in the V_{Corr} was also noted for zinc-magnesium and zinc-copper alloys. Furthermore, ternary zinc alloy was characterised by the thickest corrosion products layer and the lowest mass loss after 120h IT. A thicker layer of corrosion products was observed in the vicinity of the eutectic mixture, which can be explained by the fact that magnesium ions also release into the corrosive solution, thus facilitating the formation of subsequent products [30]. This was also confirmed by SEM observations of corrosion products. After removing the corrosion products in the ZnMgCu alloy, the eutectic mixture was exposed, which implies that it is a specific place for degradation. A more compact layer of products can protect the material from degradation, which contributed to lowering the corrosion rate of the ZnMgCu alloy. Moreover, this phenomenon can be intensified by the increased number of grain boundaries in ZnMgCu alloys. In general, grain boundaries are more reactive than grain interior, thus may facilitate ion transport and creation of protective layer [31]. Alloying additives affect mechanical properties in different ways, depending on the chemical composition. They can strengthen zinc by formation of a eutectic mixture (ZnMg and ZnMgCu) or by solid solution (ZnCu, ZnMgCu). Both of these elements affect the grain growth during casting (microstructure refinement as compared with pure Zn). What is more, all these microstructure features constitute an obstacle to the movement of dislocations during the tensile test increasing the mechanical strength. In summary, the ZnMgCu alloy with contribution of all of the mentioned strengthening mechanisms, described by the smallest grain size, with the presence of eutectic mixture and Cu dissolved in the solution, result in the best YS and UTS for this material. The low elongation of materials with the addition of Mg is a consequence of the presence of the brittle Mg_2Zn_{11} phase. However, alloying zinc with Cu increases elongation during tensile testing. Several hypotheses have been developed to explain this effect, of which the main, proposing the occurrence of twinning during deformation, is the most common [10,12,14,16,17,21].

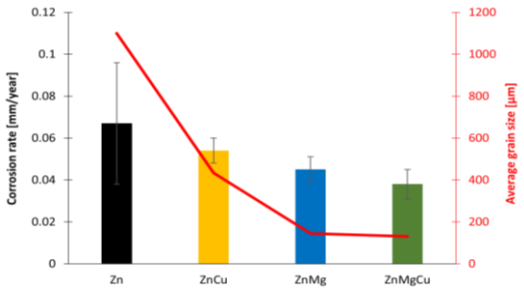

Fig. 13. Relation between grain size and corrosion rate calculated based on mass loss of the samples exposed to HBSS for 120h

5. CONCLUSIONS

Results lead to the following conclusions:

1. Alloying additives contribute to decreasing average grain size. The most favourable effect was achieved by the addition of magnesium, which formed a eutectic mixture located at α-Zn grains preventing grain growth during casting. The addition of copper has a less pronounced effect on the microstructure refinement, as all its atoms dissolved in the η-Zn grain structure.
2. The results of potentiodynamic corrosion tests suggests that the ternary ZnMgCu alloy, with a composition proposed and designed for the first time in this work, has a corrosion rate comparable to initial pure Zn material, even if any of the additive itself results in significant changes in this property.
3. Immersing the samples in HBSS solution gave more complex results as the tendencies depend on whether the samples were investigated for 24 or 120h. Longer immersion testing resulted in far lower corrosion rates compared with the first 24h. Moreover, for 120h a relation between corrosion rate and grain size was noticed. The smaller the grain size, the more corrosion resistant the material was.
4. Increased number of alloying elements affected the formation of the corrosion product layer. The thickest layer was observed for ZnMgCu, which was connected with the Mg_2Zn_{11} phase and grain refinement.
5. ZnMgCu possessed the highest mechanical strength due to the presence of magnesium facilitating the formation of eutectic mixture (with the presence of a hard but brittle Mg_2Zn_{11} intermetallic phase) allowing significant refinement of the microstructure and to copper being dissolved within the refined η-Zn grains.

6. Results indicate the effect of a particular element on microstructure as well as on mechanical and corrosion properties. Detailed characterisation of the materials in as-cast state established the unambiguous impact of alloying, which may contribute to the selection of potential material for further research in the context of application as biodegradable stents. From our results, it seems that ternary ZnMgCu is the most promising one.

ACKNOWLEDGEMENTS

This work was supported by the National Center for Research and Development, grant number LIDER/54/0229/L-11/19/NCBR/2020

REFERENCES

[1] X. Tong *et al.*, "Biodegradable Zn–Cu–Li alloys with ultrahigh strength, ductility, antibacterial ability, cytocompatibility, and suitable degradation rate for potential bone-implant applications," *Smart Materials in Manufacturing*, vol. 1, p. 100012, 2023, doi: 10.1016/j.smmf.2022.100012.

[2] X. Liu *et al.*, "Micro-alloying with Mn in Zn–Mg alloy for future biodegradable metals application," *Mater Des*, vol. 94, pp. 95–104, Mar. 2016, doi: 10.1016/j.matdes.2015.12.128.

[3] H. Gong, K. Wang, R. Strich, and J. G. Zhou, "In vitro biodegradation behavior, mechanical properties, and cytotoxicity of biodegradable Zn–Mg alloy," *J Biomed Mater Res B Appl Biomater*, vol. 103, no. 8, pp. 1632–1640, Nov. 2015, doi: 10.1002/jbm.b.33341.

[4] P. K. Bowen, J. Drelich, and J. Goldman, "Zinc Exhibits Ideal Physiological Corrosion Behavior for Bioabsorbable Stents," *Advanced Materials*, vol. 25, no. 18, pp. 2577–2582, May 2013, doi: 10.1002/adma.201300226.

[5] P. K. Bowen *et al.*, "Biodegradable Metals for Cardiovascular Stents: from Clinical Concerns to Recent Zn-Alloys," *Adv Healthc Mater*, vol. 5, no. 10, pp. 1121–1140, May 2016, doi: 10.1002/adhm.201501019.

[6] L. Kong, Z. Heydari, G. H. Lami, A. Saberi, M. S. Baltatu, and P. Vizureanu, "A Comprehensive Review of the Current Research Status of Biodegradable Zinc Alloys and Composites for Biomedical Applications," *Materials*, vol. 16, no. 13, p. 4797, Jul. 2023, doi: 10.3390/ma16134797.

[7] E. Mostaed, M. Sikora-Jasinska, J. W. Drelich, and M. Vedani, "Zinc-based alloys for degradable vascular stent applications," *Acta Biomater*, vol. 71, pp. 1–23, Apr. 2018, doi: 10.1016/j.actbio.2018.03.005.

[8] H. Kabir, K. Munir, C. Wen, and Y. Li, "Recent research and progress of biodegradable zinc alloys and composites for biomedical applications: Biomechanical and biocorrosion perspectives," *Bioact Mater*, vol. 6, no. 3, pp. 836–879, Mar. 2021, doi: 10.1016/j.bioactmat.2020.09.013.

[9] S. Liu, D. Kent, N. Doan, M. Dargusch, and G. Wang, "Effects of deformation twinning on the mechanical properties of biodegradable Zn-Mg alloys," *Bioact Mater*, vol. 4, pp. 8–16, Dec. 2019, doi: 10.1016/j.bioactmat.2018.11.001.

[10] C. Shen *et al.*, "Mechanical properties, in vitro degradation behavior, hemocompatibility and cytotoxicity evaluation of Zn–1.2Mg alloy for biodegradable implants," *RSC Adv*, vol. 6, no. 89, pp. 86410–86419, 2016, doi: 10.1039/C6RA14300H.

[11] J. Kubásek, D. Vojtěch, I. Pospíšilová, A. Michalcová, and J. Maixner, "Microstructure and mechanical properties of the micrograined hypoeutectic Zn–Mg alloy," *International Journal of Minerals, Metallurgy, and Materials*, vol. 23, no. 10, pp. 1167–1176, Oct. 2016, doi: 10.1007/s12613-016-1336-7.

[12] M. S. Dambatta, S. Izman, D. Kurniawan, and H. Hermawan, "Processing of Zn-3Mg alloy by equal channel angular pressing for biodegradable metal implants," *J King Saud Univ Sci*, vol. 29, no. 4, pp. 455–461, Oct. 2017, doi: 10.1016/j.jksus.2017.07.008.

[13] L. Ye *et al.*, "Effect of grain size and volume fraction of eutectic structure on mechanical properties and corrosion behavior of as-cast Zn–Mg binary alloys," *Journal of Materials Research and Technology*, vol. 16, pp. 1673–1685, Jan. 2022, doi: 10.1016/j.jmrt.2021.12.101.

[14] P. Li *et al.*, "Investigation of zinc-copper alloys as potential materials for craniomaxillofacial osteosynthesis implants," *Materials Science and Engineering: C*, vol. 103, p. 109826, Oct. 2019, doi: 10.1016/j.msec.2019.109826.

[15] X. Liu *et al.*, "Microstructure, mechanical properties, in vitro degradation behavior and hemocompatibility of novel Zn–Mg–Sr alloys as biodegradable metals," *Mater Lett*, vol. 162, pp. 242–245, Jan. 2016, doi: 10.1016/j.matlet.2015.07.151.

[16] L. Zhang, X. Y. Liu, H. Huang, and W. Zhan, "Effects of Ti on microstructure, mechanical properties and biodegradation behavior of Zn-Cu alloy," *Mater Lett*, vol. 244, pp. 119–122, Jun. 2019, doi: 10.1016/j.matlet.2019.02.071.

[17] X. Liu *et al.*, "Effects of alloying elements (Ca and Sr) on microstructure, mechanical property and in vitro corrosion behavior of biodegradable Zn–1.5Mg alloy," *J Alloys Compd*, vol. 664, pp. 444–452, Apr. 2016, doi: 10.1016/j.jallcom.2015.10.116.

[18] H. F. Li *et al.*, "Development of biodegradable Zn-1X binary alloys with nutrient alloying elements Mg, Ca and Sr," *Sci Rep*, vol. 5, no. 1, p. 12190, Aug. 2015, doi: 10.1038/srep12190.

[19] J. Lin *et al.*, "Biodegradable Zn–3Cu and Zn–3Cu–0.2Ti alloys with ultrahigh ductility and antibacterial ability for orthopedic applications," *J Mater Sci Technol*, vol. 68, pp. 76–90, Mar. 2021, doi: 10.1016/j.jmst.2020.06.052.

[20] M. Wątroba *et al.*, "Design of novel Zn-Ag-Zr alloy with enhanced strength as a potential biodegradable implant material," *Mater Des*, vol. 183, p. 108154, Dec. 2019, doi: 10.1016/j.matdes.2019.108154.

[21] X. Wang, Y. Ma, B. Meng, and M. Wan, "Effect of equal-channel angular pressing on microstructural evolution, mechanical property and biodegradability of an ultrafine-grained zinc alloy," *Materials Science and Engineering: A*, vol. 824, p. 141857, Sep. 2021, doi: 10.1016/j.msea.2021.141857.

[22] L. Li *et al.*, "Investigation on microstructures, mechanical properties and in vitro corrosion behavior of novel biodegradable Zn-2Cu-0.01Ti-xLi alloys," *J Alloys Compd*, vol. 888, p. 161529, Dec. 2021, doi: 10.1016/j.jallcom.2021.161529.

[23] X. Tong *et al.*, "Development of biodegradable Zn–1Mg–0.1RE (RE = Er, Dy, and Ho) alloys for biomedical applications," *Acta Biomater*, vol. 117, pp. 384–399, Nov. 2020, doi: 10.1016/j.actbio.2020.09.036.

[24] J. Lin *et al.*, "Biodegradable ternary Zn–3Ge–0.5X (X=Cu, Mg, and Fe) alloys for orthopedic applications," *Acta Biomater*, vol. 115, pp. 432–446, Oct. 2020, doi: 10.1016/j.actbio.2020.08.033.

[25] G. Katarivas Levy, J. Goldman, and E. Aghion, "The Prospects of Zinc as a Structural Material for Biodegradable Implants—A Review Paper," *Metals (Basel)*, vol. 7, no. 10, p. 402, Oct. 2017, doi: 10.3390/met7100402.

[26] S. Huang, L. Wang, Y. Zheng, L. Qiao, and Y. Yan, "In vitro degradation behavior of novel Zn–Cu–Li alloys: Roles of alloy composition and rolling processing," *Mater Des*, vol. 212, p. 110288, Dec. 2021, doi: 10.1016/j.matdes.2021.110288.

[27] C. García-Mintegui *et al.*, "Zn-Mg and Zn-Cu alloys for stenting applications: From nanoscale mechanical characterization to in vitro degradation and biocompatibility," *Bioact Mater*, vol. 6, no. 12, pp. 4430–4446, Dec. 2021, doi: 10.1016/j.bioactmat.2021.04.015.

[28] G. Bao *et al.*, "Feasibility evaluation of a Zn-Cu alloy for intrauterine devices: In vitro and in vivo studies," *Acta Biomater*, vol. 142, pp. 374–387, Apr. 2022, doi: 10.1016/j.actbio.2022.01.053.

[29] J. Huang *et al.*, "Preparation and Properties of Zn-Cu Alloy for Potential Stent Material," *J Mater Eng Perform*, vol. 29, no. 10, pp. 6484–6493, Oct. 2020, doi: 10.1007/s11665-020-05167-0.

[30] M. M. Alves, T. Prošek, C. F. Santos, and M. F. Montemor, "Evolution of the in vitro degradation of Zn–Mg alloys under simulated physiological conditions," *RSC Adv*, vol. 7, no. 45, pp. 28224–28233, 2017, doi: 10.1039/C6RA28542B.

[31] K. D. Ralston and N. Birbilis, "Effect of Grain Size on Corrosion: A Review," *CORROSION*, vol. 66, no. 7, pp. 075005-075005–13, Jul. 2010, doi: 10.5006/1.3462912.